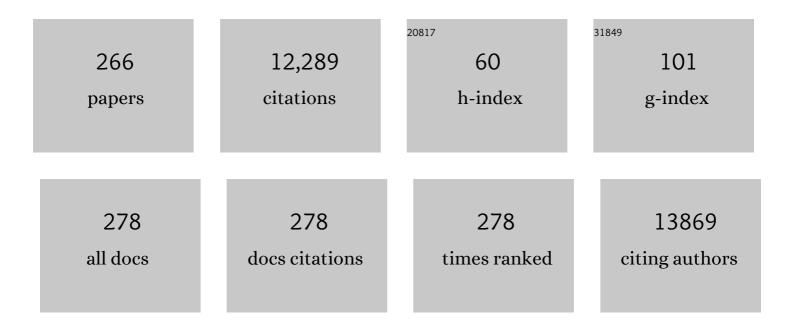
Marcel A Verheijen

List of Publications by Year in descending order

Source: https://exaly.com/author-pdf/6582492/publications.pdf Version: 2024-02-01



#	Article	IF	CITATIONS
1	Growth of PbTe nanowires by molecular beam epitaxy. Materials for Quantum Technology, 2022, 2, 015001.	3.1	13
2	Continuous-Flow Sunlight-Powered CO2 Methanation Catalyzed by γ-Al2O3-Supported Plasmonic Ru Nanorods. Catalysts, 2022, 12, 126.	3.5	9
3	Enhanced Self-Assembled Monolayer Surface Coverage by ALD NiO in p-i-n Perovskite Solar Cells. ACS Applied Materials & Interfaces, 2022, 14, 2166-2176.	8.0	77
4	Comparing the Performance of Supported Ru Nanocatalysts Prepared by Chemical Reduction of RuCl3 and Thermal Decomposition of Ru3(CO)12 in the Sunlight-Powered Sabatier Reaction. Catalysts, 2022, 12, 284.	3.5	4
5	Controlling transition metal atomic ordering in two-dimensional Mo _{1â^'x} W _x S ₂ alloys. 2D Materials, 2022, 9, 025016.	4.4	9
6	Operando Spectroscopy Unveils the Catalytic Role of Different Palladium Oxidation States in CO Oxidation on Pd/CeO ₂ Catalysts. Angewandte Chemie - International Edition, 2022, 61, .	13.8	16
7	Thickness and Morphology Dependent Electrical Properties of ALDâ€Synthesized MoS ₂ FETs. Advanced Electronic Materials, 2022, 8, .	5.1	9
8	Titelbild: Operando Spectroscopy Unveils the Catalytic Role of Different Palladium Oxidation States in CO Oxidation on Pd/CeO ₂ Catalysts (Angew. Chem. 23/2022). Angewandte Chemie, 2022, 134,	2.0	0
9	Prismatic Ge-rich inclusions in the hexagonal SiGe shell of GaP–Si–SiGe nanowires by controlled faceting. Nanoscale, 2021, 13, 9436-9445.	5.6	1
10	Surface passivation of germanium by atomic layer deposited Al2O3 nanolayers. Journal of Materials Research, 2021, 36, 571-581.	2.6	21
11	Parity-preserving and magnetic field–resilient superconductivity in InSb nanowires with Sn shells. Science, 2021, 372, 508-511.	12.6	50
12	Improved Pd/CeO ₂ Catalysts for Low-Temperature NO Reduction: Activation of CeO ₂ Lattice Oxygen by Fe Doping. ACS Catalysis, 2021, 11, 5614-5627.	11.2	44
13	Unveiling Planar Defects in Hexagonal Group IV Materials. Nano Letters, 2021, 21, 3619-3625.	9.1	8
14	Impact of Ions on Film Conformality and Crystallinity during Plasma-Assisted Atomic Layer Deposition of TiO ₂ . Chemistry of Materials, 2021, 33, 5002-5009.	6.7	16
15	On the Contact Optimization of ALD-Based MoS ₂ FETs: Correlation of Processing Conditions and Interface Chemistry with Device Electrical Performance. ACS Applied Electronic Materials, 2021, 3, 3185-3199.	4.3	8
16	Universal Platform for Scalable Semiconductor‧uperconductor Nanowire Networks. Advanced Functional Materials, 2021, 31, 2103062.	14.9	10
17	Phase separation of VO2 and SiO2 on SiO2-Coated float glass yields robust thermochromic coating with unrivalled optical properties. Solar Energy Materials and Solar Cells, 2021, 230, 111238.	6.2	7
18	Low Temperature Sunlightâ€Powered Reduction of CO ₂ to CO Using a Plasmonic Au/TiO ₂ Nanocatalyst. ChemCatChem, 2021, 13, 4507-4513.	3.7	15

#	Article	IF	CITATIONS
19	Novel microreactor and generic model catalyst platform for the study of fast temperature pulsed operation $\hat{a} \in CO$ oxidation rate enhancement on Pt. Chemical Engineering Journal, 2021, 425, 131559.	12.7	2
20	Atomic-layer-deposited Al-doped zinc oxide as a passivating conductive contacting layer for n+-doped surfaces in silicon solar cells. Solar Energy Materials and Solar Cells, 2021, 233, 111386.	6.2	28
21	Conformal Growth of Nanometer-Thick Transition Metal Dichalcogenide TiS <i>_x</i> -NbS <i>_x</i> Heterostructures over 3D Substrates by Atomic Layer Deposition: Implications for Device Fabrication. ACS Applied Nano Materials, 2021, 4, 514-521.	5.0	8
22	Excellent surface passivation of germanium by a-Si:H/Al2O3 stacks. Journal of Applied Physics, 2021, 130,	2.5	14
23	Probing the Origin and Suppression of Vertically Oriented Nanostructures of 2D WS ₂ Layers. ACS Applied Materials & Interfaces, 2020, 12, 3873-3885.	8.0	22
24	Hard Superconducting Gap and Diffusion-Induced Superconductors in Ge–Si Nanowires. Nano Letters, 2020, 20, 122-130.	9.1	18
25	Atomic layer deposition of ruthenium using an ABC-type process: Role of oxygen exposure during nucleation. Journal of Vacuum Science and Technology A: Vacuum, Surfaces and Films, 2020, 38, .	2.1	8
26	Collective photothermal effect of Al ₂ O ₃ â€supported spheroidal plasmonic Ru nanoparticle catalysts in the sunlightâ€powered Sabatier reaction. ChemCatChem, 2020, 12, 5618-5622.	3.7	24
27	Area-Selective Atomic Layer Deposition of TiN Using Aromatic Inhibitor Molecules for Metal/Dielectric Selectivity. Chemistry of Materials, 2020, 32, 7788-7795.	6.7	42
28	Synthesis of edge-enriched WS2 on high surface area WS2 framework by atomic layer deposition for electrocatalytic hydrogen evolution reaction. Journal of Vacuum Science and Technology A: Vacuum, Surfaces and Films, 2020, 38, .	2.1	4
29	Atomic Layer Deposition of Al-Doped MoS ₂ : Synthesizing a p-type 2D Semiconductor with Tunable Carrier Density. ACS Applied Nano Materials, 2020, 3, 10200-10208.	5.0	22
30	Probing Lattice Dynamics and Electronic Resonances in Hexagonal Ge and Si _{<i>x</i>} Ge _{1–<i>x</i>} Alloys in Nanowires by Raman Spectroscopy. ACS Nano, 2020, 14, 6845-6856.	14.6	17
31	Ballistic Phonons in Ultrathin Nanowires. Nano Letters, 2020, 20, 2703-2709.	9.1	30
32	Extraction of Dzyaloshinskii-Moriya interaction from propagating spin waves. Physical Review B, 2020, 101, .	3.2	21
33	Large area, patterned growth of 2D MoS ₂ and lateral MoS ₂ –WS ₂ heterostructures for nano- and opto-electronic applications. Nanotechnology, 2020, 31, 255603.	2.6	46
34	Atomic layer deposition of Nb-doped TiO2: Dopant incorporation and effect of annealing. Journal of Vacuum Science and Technology A: Vacuum, Surfaces and Films, 2020, 38, .	2.1	12
35	Kinetic Control of Morphology and Composition in Ge/GeSn Core/Shell Nanowires. ACS Nano, 2020, 14, 2445-2455.	14.6	17
36	Editorial Expression of Concern: Quantized Majorana conductance. Nature, 2020, 581, E4-E4.	27.8	10

#	Article	IF	CITATIONS
37	Area-Selective Atomic Layer Deposition of Two-Dimensional WS ₂ Nanolayers. , 2020, 2, 511-518.		45
38	Direct-bandgap emission from hexagonal Ge and SiGe alloys. Nature, 2020, 580, 205-209.	27.8	231
39	In-plane selective area InSb–Al nanowire quantum networks. Communications Physics, 2020, 3, .	5.3	37
40	Understanding the Film Formation Kinetics of Sequential Deposited Narrowâ€Bandgap Pb–Sn Hybrid Perovskite Films. Advanced Energy Materials, 2020, 10, 2000566.	19.5	33
41	Plasma-Assisted ALD of Highly Conductive HfNx: On the Effect of Energetic Ions on Film Microstructure. Plasma Chemistry and Plasma Processing, 2020, 40, 697-712.	2.4	13
42	Precise ion energy control with tailored waveform biasing for atomic scale processing. Journal of Applied Physics, 2020, 128, .	2.5	26
43	Full characterization and modeling of graded interfaces in a high lattice-mismatch axial nanowire heterostructure. Physical Review Materials, 2020, 4, .	2.4	5
44	Towards a Hexagonal SiGe Semiconductor Laser , 2020, , .		0
45	Transition Matrix Element and Recombination Mechanism of Hexagonal SiGe , 2020, , .		0
46	Transition in layer structure of atomic/molecular layer deposited ZnO-zincone multilayers. Journal of Vacuum Science and Technology A: Vacuum, Surfaces and Films, 2019, 37, .	2.1	9
47	Low-Temperature Phase-Controlled Synthesis of Titanium Di- and Tri-sulfide by Atomic Layer Deposition. Chemistry of Materials, 2019, 31, 9354-9362.	6.7	35
48	Strain engineering in Ge/GeSn core/shell nanowires. Applied Physics Letters, 2019, 115, .	3.3	22
49	21.6%-Efficient Monolithic Perovskite/Cu(In,Ga)Se ₂ Tandem Solar Cells with Thin Conformal Hole Transport Layers for Integration on Rough Bottom Cell Surfaces. ACS Energy Letters, 2019, 4, 583-590.	17.4	155
50	Area-Selective Atomic Layer Deposition of ZnO by Area Activation Using Electron Beam-Induced Deposition. Chemistry of Materials, 2019, 31, 1250-1257.	6.7	62
51	Area-Selective Deposition of Ruthenium by Combining Atomic Layer Deposition and Selective Etching. Chemistry of Materials, 2019, 31, 3878-3882.	6.7	71
52	Phonon Engineering in Twinning Superlattice Nanowires. Nano Letters, 2019, 19, 4702-4711.	9.1	31
53	Edge-Site Nanoengineering of WS ₂ by Low-Temperature Plasma-Enhanced Atomic Layer Deposition for Electrocatalytic Hydrogen Evolution. Chemistry of Materials, 2019, 31, 5104-5115.	6.7	57
54	Boosting the Performance of WO ₃ /n‣i Heterostructures for Photoelectrochemical Water Splitting: from the Role of Si to Interface Engineering. Advanced Energy Materials, 2019, 9, 1900940.	19.5	48

#	Article	IF	CITATIONS
55	Electrochemistry of Sputtered Hematite Photoanodes: A Comparison of Metallic DC versus Reactive RF Sputtering. ACS Omega, 2019, 4, 9262-9270.	3.5	7
56	High Mobility Stemless InSb Nanowires. Nano Letters, 2019, 19, 3575-3582.	9.1	36
57	Sunlight-Fueled, Low-Temperature Ru-Catalyzed Conversion of CO ₂ and H ₂ to CH ₄ with a High Photon-to-Methane Efficiency. ACS Omega, 2019, 4, 7369-7377.	3.5	28
58	Hexagonal silicon grown from higher order silanes. Nanotechnology, 2019, 30, 295602.	2.6	12
59	Bottomâ€Up Grown 2D InSb Nanostructures. Advanced Materials, 2019, 31, e1808181.	21.0	26
60	Polarized Raman spectroscopy to elucidate the texture of synthesized MoS ₂ . Nanoscale, 2019, 11, 22860-22870.	5.6	13
61	Plasma-assisted atomic layer deposition of nickel oxide as hole transport layer for hybrid perovskite solar cells. Journal of Materials Chemistry C, 2019, 7, 12532-12543.	5.5	80
62	Chemical Analysis of the Interface between Hybrid Organic–Inorganic Perovskite and Atomic Layer Deposited Al ₂ O ₃ . ACS Applied Materials & Interfaces, 2019, 11, 5526-5535.	8.0	40
63	Selective-area chemical beam epitaxy of in-plane InAs one-dimensional channels grown on InP(001), InP(111)B, and InP(011) surfaces. Physical Review Materials, 2019, 3, .	2.4	48
64	Low-temperature plasma-enhanced atomic layer deposition of 2-D MoS ₂ : large area, thickness control and tuneable morphology. Nanoscale, 2018, 10, 8615-8627.	5.6	90
65	Low resistivity HfN _x grown by plasma-assisted ALD with external rf substrate biasing. Journal of Materials Chemistry C, 2018, 6, 3917-3926.	5.5	31
66	Dopant Distribution in Atomic Layer Deposited ZnO:Al Films Visualized by Transmission Electron Microscopy and Atom Probe Tomography. Chemistry of Materials, 2018, 30, 1209-1217.	6.7	28
67	Shape and structural motifs control of MgTi bimetallic nanoparticles using hydrogen and methane as trace impurities. Nanoscale, 2018, 10, 1297-1307.	5.6	4
68	Efficient Green Emission from Wurtzite Al _{<i>x</i>} In _{1–<i>x</i>} P Nanowires. Nano Letters, 2018, 18, 3543-3549.	9.1	16
69	Surface Fluorination of ALD TiO ₂ Electron Transport LayerÂfor Efficient Planar Perovskite Solar Cells. Advanced Materials Interfaces, 2018, 5, 1701456.	3.7	27
70	Bottom-up meets top-down: tailored raspberry-like Fe ₃ O ₄ –Pt nanocrystal superlattices. Nanoscale, 2018, 10, 5859-5863.	5.6	4
71	Tuning Material Properties of Oxides and Nitrides by Substrate Biasing during Plasma-Enhanced Atomic Layer Deposition on Planar and 3D Substrate Topographies. ACS Applied Materials & Interfaces, 2018, 10, 13158-13180.	8.0	85
72	Critical strain for Sn incorporation into spontaneously graded Ge/GeSn core/shell nanowires. Nanoscale, 2018, 10, 7250-7256.	5.6	28

#	Article	IF	CITATIONS
73	Spin–Orbit Interaction and Induced Superconductivity in a One-Dimensional Hole Gas. Nano Letters, 2018, 18, 6483-6488.	9.1	22
74	lsotropic Atomic Layer Etching of ZnO Using Acetylacetone and O ₂ Plasma. ACS Applied Materials & Interfaces, 2018, 10, 38588-38595.	8.0	30
75	Qualification of an Ultrasonic Instrument for Real-Time Monitoring of Size and Concentration of Nanoparticles during Liquid Phase Bottom-Up Synthesis. Applied Sciences (Switzerland), 2018, 8, 1064.	2.5	4
76	Physical and Chemical Defects in WO ₃ Thin Films and Their Impact on Photoelectrochemical Water Splitting. ACS Applied Energy Materials, 2018, 1, 5887-5895.	5.1	53
77	Atomic-layer deposited Nb2O5 as transparent passivating electron contact for c-Si solar cells. Solar Energy Materials and Solar Cells, 2018, 184, 98-104.	6.2	64
78	Twofold origin of strain-induced bending in core–shell nanowires: the GaP/InGaP case. Nanotechnology, 2018, 29, 315703.	2.6	17
79	Flow Cell Coupled Dynamic Light Scattering for Real-Time Monitoring of Nanoparticle Size during Liquid Phase Bottom-Up Synthesis. Applied Sciences (Switzerland), 2018, 8, 108.	2.5	8
80	Low-Temperature Plasma-Assisted Atomic-Layer-Deposited SnO ₂ as an Electron Transport Layer in Planar Perovskite Solar Cells. ACS Applied Materials & Interfaces, 2018, 10, 30367-30378.	8.0	88
81	Decoupling high surface recombination velocity and epitaxial growth for silicon passivation layers on crystalline silicon. Journal Physics D: Applied Physics, 2017, 50, 065305.	2.8	4
82	Towards the implementation of atomic layer deposited In2O3:H in silicon heterojunction solar cells. Solar Energy Materials and Solar Cells, 2017, 163, 43-50.	6.2	32
83	Plasma-assisted atomic layer deposition of conformal Pt films in high aspect ratio trenches. Journal of Chemical Physics, 2017, 146, 052818.	3.0	17
84	Atomic layer deposition of HfO2 using HfCp(NMe2)3 and O2 plasma. Journal of Vacuum Science and Technology A: Vacuum, Surfaces and Films, 2017, 35, .	2.1	32
85	Uniform Atomic Layer Deposition of Al ₂ O ₃ on Graphene by Reversible Hydrogen Plasma Functionalization. Chemistry of Materials, 2017, 29, 2090-2100.	6.7	64
86	Plasma-assisted atomic layer deposition of HfNx: Tailoring the film properties by the plasma gas composition. Journal of Vacuum Science and Technology A: Vacuum, Surfaces and Films, 2017, 35, .	2.1	9
87	Boosting Hole Mobility in Coherently Strained [110]-Oriented Ge–Si Core–Shell Nanowires. Nano Letters, 2017, 17, 2259-2264.	9.1	51
88	Atomic layer deposition for perovskite solar cells: research status, opportunities and challenges. Sustainable Energy and Fuels, 2017, 1, 30-55.	4.9	150
89	Growth and Optical Properties of Direct Band Gap Ge/Ge _{0.87} Sn _{0.13} Core/Shell Nanowire Arrays. Nano Letters, 2017, 17, 1538-1544.	9.1	72
90	Atomic Layer Deposition of In ₂ O ₃ :H from InCp and H ₂ O/O ₂ : Microstructure and Isotope Labeling Studies. ACS Applied Materials & Interfaces, 2017, 9, 592-601.	8.0	21

#	Article	IF	CITATIONS
91	Electrically conductive coatings consisting of Ag-decorated cellulose nanocrystals. Cellulose, 2017, 24, 2191-2204.	4.9	30
92	Synthesis of single-walled carbon nanotubes from atomic-layer-deposited Co3O4 and Co3O4/Fe2O3 catalyst films. Carbon, 2017, 121, 389-398.	10.3	18
93	Atomic layer deposition of high-mobility hydrogen-doped zinc oxide. Solar Energy Materials and Solar Cells, 2017, 173, 111-119.	6.2	40
94	Dynamic reconfiguration of van der Waals gaps within GeTe–Sb ₂ Te ₃ based superlattices. Nanoscale, 2017, 9, 8774-8780.	5.6	71
95	Microscopic studies of polycrystalline nanoparticle growth in free space. Journal of Crystal Growth, 2017, 467, 137-144.	1.5	3
96	Improved structural and electrical properties in native Sb2Te3/GexSb2Te3+x van der Waals superlattices due to intermixing mitigation. APL Materials, 2017, 5, .	5.1	26
97	Protecting patches in colloidal synthesis of Au semishells. Chemical Communications, 2017, 53, 3898-3901.	4.1	5
98	Single-Crystalline Hexagonal Silicon–Germanium. Nano Letters, 2017, 17, 85-90.	9.1	59
99	Atomic layer deposition of highly dispersed Pt nanoparticles on a high surface area electrode backbone for electrochemical promotion of catalysis. Electrochemistry Communications, 2017, 84, 40-44.	4.7	17
100	(Invited) Area-Selective Atomic Layer Deposition: Role of Surface Chemistry. ECS Transactions, 2017, 80, 39-48.	0.5	13
101	Effective Surface Passivation of InP Nanowires by Atomic-Layer-Deposited Al ₂ O ₃ with PO _{<i>x</i>/i>} Interlayer. Nano Letters, 2017, 17, 6287-6294.	9.1	68
102	Crystal Phase Quantum Well Emission with Digital Control. Nano Letters, 2017, 17, 6062-6068.	9.1	27
103	Surface passivation of <i>n</i> -type doped black silicon by atomic-layer-deposited SiO2/Al2O3 stacks. Applied Physics Letters, 2017, 110, .	3.3	18
104	The Influence of Particle Size Distribution and Shell Imperfections on the Plasmon Resonance of Au and Ag Nanoshells. Plasmonics, 2017, 12, 929-945.	3.4	20
105	High-efficiency humidity-stable planar perovskite solar cells based on atomic layer architecture. Energy and Environmental Science, 2017, 10, 91-100.	30.8	231
106	Synthesis of Polystyrene–Polyphenylsiloxane Janus Particles through Colloidal Assembly with Unexpected High Selectivity: Mechanistic Insights and Their Application in the Design of Polystyrene Particles with Multiple Polyphenylsiloxane Patches. Polymers, 2017, 9, 475.	4.5	8
107	Synthesis and Characterization of Hybrid Particles Obtained in a One-Pot Process through Simultaneous Sol-Gel Reaction of (3-Mercaptopropyl)trimethoxysilane and Emulsion Polymerization of Styrene. Colloids and Interfaces, 2017, 1, 7.	2.1	3
108	Atomic-layer deposited passivation schemes for c-Si solar cells. , 2017, , .		4

108 Atomic-layer deposited passivation schemes for c-Si solar cells. , 2017, , .

7

#	Article	IF	CITATIONS
109	Silicon heterojunction solar cell passivation in combination with nanocrystalline silicon oxide emitters. Physica Status Solidi (A) Applications and Materials Science, 2016, 213, 1932-1936.	1.8	9
110	Receptor-Targeted Luminescent Silver Bionanoparticles. European Journal of Inorganic Chemistry, 2016, 2016, 3030-3035.	2.0	4
111	Pseudodirect to Direct Compositional Crossover in Wurtzite GaP/In _{<i>x</i>} Ga _{1–<i>x</i>} P Core–Shell Nanowires. Nano Letters, 2016, 16, 7930-7936.	9.1	19
112	Atomic-layer deposited passivation schemes for c-Si solar cells. , 2016, , .		3
113	Atomic stacking and van-der-Waals bonding in GeTe–Sb ₂ Te ₃ superlattices. Journal of Materials Research, 2016, 31, 3115-3124.	2.6	53
114	On the solid phase crystallization of In2O3:H transparent conductive oxide films prepared by atomic layer deposition. Journal of Applied Physics, 2016, 120, .	2.5	27
115	Crossed InSb nanowire junctions for Majorana operations. , 2016, , .		0
116	Strong reduction of spectral heterogeneity in gold bipyramids for single-particle and single-molecule plasmon sensing. Nanotechnology, 2016, 27, 024001.	2.6	18
117	High-Yield Growth and Characterization of ⟠100⟩ InP p–n Diode Nanowires. Nano Letters, 2016, 16, 3071-3077.	9.1	11
118	Gas phase grown silicon germanium nanocrystals. Chemical Physics Letters, 2016, 661, 185-190.	2.6	3
119	On the Growth, Percolation and Wetting of Silver Thin Films Grown by Atmospheric-Plasma Enhanced Spatial Atomic Layer Deposition. ECS Transactions, 2016, 75, 129-142.	0.5	6
120	Impurity and Defect Monitoring in Hexagonal Si and SiGe Nanocrystals. ECS Transactions, 2016, 75, 751-760.	0.5	6
121	Expanding Thermal Plasma Deposition of Alâ€Đoped ZnO: On the Effect of the Plasma Chemistry on Film Growth Mechanisms. Plasma Processes and Polymers, 2016, 13, 54-69.	3.0	5
122	The competing roles of i-ZnO in Cu(In,Ga)Se2 solar cells. Solar Energy Materials and Solar Cells, 2016, 157, 798-807.	6.2	21
123	Influence of growth conditions on the performance of InP nanowire solar cells. Nanotechnology, 2016, 27, 454003.	2.6	10
124	New opportunities with nanowires. , 2016, , .		0
125	Ordered Peierls distortion prevented at growth onset of GeTe ultra-thin films. Scientific Reports, 2016, 6, 32895.	3.3	20
126	Revisiting the Local Structure in Ge-Sb-Te based Chalcogenide Superlattices. Scientific Reports, 2016, 6, 22353.	3.3	63

#	Article	IF	CITATIONS
127	Surface Infrared Spectroscopy during Low Temperature Growth of Supported Pt Nanoparticles by Atomic Layer Deposition. Journal of Physical Chemistry C, 2016, 120, 750-755.	3.1	20
128	Functional nickel-based deposits synthesized by focused beam induced processing. Nanotechnology, 2016, 27, 065303.	2.6	8
129	Atomic layer deposition of Pd and Pt nanoparticles for catalysis: on the mechanisms of nanoparticle formation. Nanotechnology, 2016, 27, 034001.	2.6	86
130	Nucleation of microcrystalline silicon: on the effect of the substrate surface nature and nano-imprint topography. Journal Physics D: Applied Physics, 2016, 49, 055205.	2.8	3
131	p-type nc-SiOx:H emitter layer for silicon heterojunction solar cells grown by rf-PECVD. Materials Research Society Symposia Proceedings, 2015, 1770, 7-12.	0.1	1
132	Sub-nanometer dimensions control of core/shell nanoparticles prepared by atomic layer deposition. Nanotechnology, 2015, 26, 094002.	2.6	60
133	Atomic layer deposition of B-doped ZnO using triisopropyl borate as the boron precursor and comparison with Al-doped ZnO. Journal of Materials Chemistry C, 2015, 3, 3095-3107.	5.5	48
134	Nitrogen-doping of bulk and nanotubular TiO2 photocatalysts by plasma-assisted atomic layer deposition. Applied Surface Science, 2015, 330, 476-486.	6.1	24
135	Hexagonal Silicon Realized. Nano Letters, 2015, 15, 5855-5860.	9.1	142
136	Efficient water reduction with gallium phosphide nanowires. Nature Communications, 2015, 6, 7824.	12.8	123
137	Asymmetric magnetic bubble expansion under in-plane field in Pt/Co/Pt: Effect of interface engineering. Physical Review B, 2015, 91, .	3.2	106
138	Encapsulation method for atom probe tomography analysis of nanoparticles. Ultramicroscopy, 2015, 159, 420-426.	1.9	40
139	Cracking the Si Shell Growth in Hexagonal GaP-Si Core–Shell Nanowires. Nano Letters, 2015, 15, 2974-2979.	9.1	23
140	Interface formation of two- and three-dimensionally bonded materials in the case of GeTe–Sb ₂ Te ₃ superlattices. Nanoscale, 2015, 7, 19136-19143.	5.6	145
141			
	Correlative transmission electron microscopy and electrical properties study of switchable phase-change random access memory line cells. Journal of Applied Physics, 2015, 117, 064504.	2.5	5
142	Correlative transmission electron microscopy and electrical properties study of switchable phase-change random access memory line cells. Journal of Applied Physics, 2015, 117, 064504. Highly porous, ultra-low refractive index coatings produced through random packing of silicated cellulose nanocrystals. Colloids and Surfaces A: Physicochemical and Engineering Aspects, 2015, 487, 1-8.	2.5 4.7	5 19
142 143	phase-change random access memory line cells. Journal of Applied Physics, 2015, 117, 064504. Highly porous, ultra-low refractive index coatings produced through random packing of silicated cellulose nanocrystals. Colloids and Surfaces A: Physicochemical and Engineering Aspects, 2015, 487,		

#	Article	IF	CITATIONS
145	Direct band gap wurtzite GaP nanowires for LEDs and quantum devices. Proceedings of SPIE, 2014, , .	0.8	0
146	Investigation of Embedded Perovskite Nanoparticles for Enhanced Capacitor Permittivities. ACS Applied Materials & Interfaces, 2014, 6, 19737-19743.	8.0	3
147	Glucose-functionalized polystyrene particles designed for selective deposition of silver on the surface. RSC Advances, 2014, 4, 62878-62881.	3.6	19
148	Plasmaâ€Assisted Atomic Layer Deposition of PtO _{<i>x</i>} from (MeCp)PtMe ₃ and O ₂ Plasma. Chemical Vapor Deposition, 2014, 20, 258-268.	1.3	11
149	Rational Design: Rationally Designed Singleâ€Crystalline Nanowire Networks (Adv. Mater. 28/2014). Advanced Materials, 2014, 26, 4908-4908.	21.0	1
150	Electrocatalytic activity of atomic layer deposited Pt–Ru catalysts onto N-doped carbon nanotubes. Journal of Catalysis, 2014, 311, 481-486.	6.2	51
151	Photoelectrochemical Hydrogen Production on InP Nanowire Arrays with Molybdenum Sulfide Electrocatalysts. Nano Letters, 2014, 14, 3715-3719.	9.1	106
152	Atomic Layer Deposition of Highly Transparent Platinum Counter Electrodes for Metal/Polymer Flexible Dyeâ€ S ensitized Solar Cells. Advanced Energy Materials, 2014, 4, 1300831.	19.5	28
153	Rationally Designed Single rystalline Nanowire Networks. Advanced Materials, 2014, 26, 4875-4879.	21.0	62
154	Atomic Layer Deposition of High-Purity Palladium Films from Pd(hfac) ₂ and H ₂ and O ₂ Plasmas. Journal of Physical Chemistry C, 2014, 118, 8702-8711.	3.1	62
155	Facile and Versatile Platform Approach for the Synthesis of Submicrometer-Sized Hybrid Particles with Programmable Size, Composition, and Architecture Comprising Organosiloxanes and/or Organosilsesquioxanes. Chemistry of Materials, 2014, 26, 5718-5724.	6.7	7
156	Compositional and Structural Analysis of Al-doped ZnO Multilayers by LEAP. Microscopy and Microanalysis, 2014, 20, 526-527.	0.4	2
157	Reversible Switching of InP Nanowire Growth Direction by Catalyst Engineering. Nano Letters, 2013, 13, 3802-3806.	9.1	107
158	Electrical transport and Al doping efficiency in nanoscale ZnO films prepared by atomic layer deposition. Journal of Applied Physics, 2013, 114, .	2.5	67
159	Formation and electronic properties of InSb nanocrosses. Nature Nanotechnology, 2013, 8, 859-864.	31.5	115
160	Efficiency Enhancement of InP Nanowire Solar Cells by Surface Cleaning. Nano Letters, 2013, 13, 4113-4117.	9.1	134
161	High optical quality single crystal phase wurtzite and zincblende InP nanowires. Nanotechnology, 2013, 24, 115705.	2.6	59
162	Room Temperature Sensing of O ₂ and CO by Atomic Layer Deposition Prepared ZnO Films Coated with Pt Nanoparticles. ECS Transactions, 2013, 58, 203-214.	0.5	4

#	Article	IF	CITATIONS
163	Wurtzite Gallium Phosphide has a direct-band gap. , 2013, , .		2
164	Ultrahigh throughput plasma processing of free standing silicon nanocrystals with lognormal size distribution. Journal of Applied Physics, 2013, 113, .	2.5	36
165	Direct Band Gap Wurtzite Gallium Phosphide Nanowires. Nano Letters, 2013, 13, 1559-1563.	9.1	262
166	Influence of Oxygen Exposure on the Nucleation of Platinum Atomic Layer Deposition: Consequences for Film Growth, Nanopatterning, and Nanoparticle Synthesis. Chemistry of Materials, 2013, 25, 1905-1911.	6.7	123
167	Tuning structural motifs and alloying of bulk immiscible Mo–Cu bimetallic nanoparticles by gas-phase synthesis. Nanoscale, 2013, 5, 5375.	5.6	56
168	Direct-Write Atomic Layer Deposition of High-Quality Pt Nanostructures: Selective Growth Conditions and Seed Layer Requirements. Journal of Physical Chemistry C, 2013, 117, 10788-10798.	3.1	58
169	Crystallization Study by Transmission Electron Microscopy of SrTiO3 Thin Films Prepared by Plasma-Assisted ALD. ECS Transactions, 2013, 50, 69-77.	0.5	2
170	Crystallization Study by Transmission Electron Microscopy of SrTiO ₃ Thin Films Prepared by Plasma-Assisted ALD. ECS Journal of Solid State Science and Technology, 2013, 2, N120-N124.	1.8	11
171	InP nanowire array solar cell with cleaned sidewalls. , 2013, , .		0
172	ALD of SrTiO ₃ and Pt for Pt/SrTiO ₃ /Pt MIM Structures: Growth and Crystallization Study. ECS Transactions, 2013, 58, 153-162.	0.5	3
173	Direct measurement of the near-field super resolved focused spot in InSb. Optics Express, 2012, 20, 10426.	3.4	20
174	Solid-phase crystallization of ultra high growth rate amorphous silicon films. Journal of Applied Physics, 2012, 111, 103510.	2.5	8
175	Growth and optical properties of axial hybrid III–V/silicon nanowires. Nature Communications, 2012, 3, 1266.	12.8	105
176	Improved conductivity of aluminum-doped ZnO: The effect of hydrogen diffusion from a hydrogenated amorphous silicon capping layer. Journal of Applied Physics, 2012, 111, 063715.	2.5	9
177	Controlling the resistivity gradient in aluminum-doped zinc oxide grown by plasma-enhanced chemical vapor deposition. Journal of Applied Physics, 2012, 112, .	2.5	9
178	Nanostructure–property relations for phaseâ€change random access memory (PCRAM) line cells. Physica Status Solidi (B): Basic Research, 2012, 249, 1972-1977.	1.5	7
179	Bright single-photon sources in bottom-up tailored nanowires. Nature Communications, 2012, 3, 737.	12.8	365
180	Supported Core/Shell Bimetallic Nanoparticles Synthesis by Atomic Layer Deposition. Chemistry of Materials, 2012, 24, 2973-2977.	6.7	142

#	ARTICLE	IF	CITATIONS
181	Position-controlled [100] InP nanowire arrays. Applied Physics Letters, 2012, 100, 053107.	3.3	62
182	Real time in situ spectroscopic ellipsometry of the growth and plasmonic properties of au nanoparticles on SiO2. Nano Research, 2012, 5, 513-520.	10.4	37
183	From InSb Nanowires to Nanocubes: Looking for the Sweet Spot. Nano Letters, 2012, 12, 1794-1798.	9.1	109
184	In situ crystallization kinetics studies of plasma-deposited, hydrogenated amorphous silicon layers. Journal of Applied Physics, 2012, 111, 033508.	2.5	9
185	Formation of Wurtzite InP Nanowires Explained by Liquid-Ordering. Nano Letters, 2011, 11, 44-48.	9.1	22
186	Crystal Structure Transfer in Core/Shell Nanowires. Nano Letters, 2011, 11, 1690-1694.	9.1	93
187	The Role of Surface Energies and Chemical Potential during Nanowire Growth. Nano Letters, 2011, 11, 1259-1264.	9.1	92
188	Enhanced field-driven domain-wall motion in Pt/Co68B32/Pt strips. Applied Physics Letters, 2011, 98, .	3.3	19
189	Plasma-Assisted Deposition of Au/SiO2 Multi-layers as Surface Plasmon Resonance-Based Red-Colored Coatings. Plasmonics, 2011, 6, 255-260.	3.4	14
190	Controlling the fixed charge and passivation properties of Si(100)/Al2O3 interfaces using ultrathin SiO2 interlayers synthesized by atomic layer deposition. Journal of Applied Physics, 2011, 110, .	2.5	150
191	III-Phospide Nanowires. , 2011, , 43-67.		0
192	Zirconia thin film preparation by wet chemical methods at low temperature. Thin Solid Films, 2010, 519, 630-634.	1.8	14
193	Quantitative prediction of junction leakage in bulk-technology CMOS devices. Solid-State Electronics, 2010, 54, 243-251.	1.4	22
194	Generic nano-imprint process for fabrication of nanowire arrays. Nanotechnology, 2010, 21, 065305.	2.6	70
195	Detection of the Presence of Gold Nanoparticles in Organs by Transmission Electron Microscopy. Materials, 2010, 3, 4681-4694.	2.9	35
196	Surface passivated InAs/InP core/shell nanowires. Semiconductor Science and Technology, 2010, 25, 024011.	2.0	92
197	Paired Twins and {112i} Morphology in GaP Nanowires. Nano Letters, 2010, 10, 2349-2356.	9.1	41

#	Article	IF	CITATIONS
199	Growth of scandium aluminum nitride nanowires on ScN(111) films on 6H‧iC substrates by HVPE. Physica Status Solidi (A) Applications and Materials Science, 2009, 206, 2809-2815.	1.8	7
200	Orientationâ€Dependent Opticalâ€Polarization Properties of Single Quantum Dots in Nanowires. Small, 2009, 5, 2134-2138.	10.0	33
201	ScAlN nanowires: A cathodoluminescence study. Journal of Crystal Growth, 2009, 311, 3147-3151.	1.5	14
202	Selective Excitation and Detection of Spin States in a Single Nanowire Quantum Dot. Nano Letters, 2009, 9, 1989-1993.	9.1	79
203	Zinc Incorporation via the Vaporâ^'Liquidâ^'Solid Mechanism into InP Nanowires. Journal of the American Chemical Society, 2009, 131, 4578-4579.	13.7	41
204	Twinning superlattices in indium phosphide nanowires. Nature, 2008, 456, 369-372.	27.8	625
205	Ultrahigh Capacitance Density for Multiple ALD-Grown MIM Capacitor Stacks in 3-D Silicon. IEEE Electron Device Letters, 2008, 29, 740-742.	3.9	130
206	Epitaxial Growth of III-V Nanowires on Group IV Substrates. Materials Research Society Symposia Proceedings, 2008, 1068, 1.	0.1	8
207	F+ implants in crystalline Si: the Si interstitial contribution. Materials Research Society Symposia Proceedings, 2008, 1070, 1.	0.1	0
208	Evolution of fluorine and boron profiles during annealing in crystalline Si. Journal of Vacuum Science & Technology B, 2008, 26, 377.	1.3	3
209	Si interstitial contribution of F+ implants in crystalline Si. Journal of Applied Physics, 2008, 103, .	2.5	1
210	Epitaxial Growth of III-V Nanowires on Group IV Substrates. MRS Bulletin, 2007, 32, 117-122.	3.5	95
211	Analysis of the Degradation Mechanism during Repeated Overwrite of Phase-Change Discs. Japanese Journal of Applied Physics, 2007, 46, 1037-1041.	1.5	0
212	Towards vertical III-V nanowire devices on silicon. Device Research Conference, IEEE Annual, 2007, , .	0.0	1
213	Towards vertical III-V nanowire devices. , 2007, , .		0
214	Three-Dimensional Morphology of GaPâ^'GaAs Nanowires Revealed by Transmission Electron Microscopy Tomography. Nano Letters, 2007, 7, 3051-3055.	9.1	87
215	Remote p-Doping of InAs Nanowires. Nano Letters, 2007, 7, 1144-1148.	9.1	70
216	Single Quantum Dot Nanowire LEDs. Nano Letters, 2007, 7, 367-371.	9.1	349

#	Article	IF	CITATIONS
217	Growth Kinetics of Heterostructured GaPâ^'GaAs Nanowires. Journal of the American Chemical Society, 2006, 128, 1353-1359.	13.7	182
218	Position-controlled epitaxial III–V nanowires on silicon. Nanotechnology, 2006, 17, S271-S275.	2.6	116
219	Dedicated FIB Preparation for TEM Cross-section Samples of Nanowires Grown Vertically on Silicon Substrates. Microscopy and Microanalysis, 2006, 12, 504-505.	0.4	0
220	Electrical and structural characterization of PLD grown CeO2–HfO2 laminated high-k gate dielectrics. Materials Science in Semiconductor Processing, 2006, 9, 1061-1064.	4.0	11
221	In situ transmission electron microscopy observations of individually selected freestanding carbon nanotubes during field emission. Ultramicroscopy, 2006, 106, 902-908.	1.9	7
222	Interface study on heterostructured GaP–GaAs nanowires. Nanotechnology, 2006, 17, 4010-4013.	2.6	60
223	Characterization of Laminated CeO[sub 2]–HfO[sub 2] High-k Gate Dielectrics Grown by Pulsed Laser Deposition. Journal of the Electrochemical Society, 2006, 153, F233.	2.9	13
224	Epitaxial III-V Nanowires on Silicon for Vertical Devices. ECS Transactions, 2006, 3, 415-423.	0.5	1
225	Laminated CeO2/HfO2 High-K Gate Dielectrics Grown by Pulsed Laser Deposition in Reducing Ambient. ECS Transactions, 2006, 3, 521-533.	0.5	2
226	Archival-overwrite performance of GeSnSb-based phase-change discs. Journal of Applied Physics, 2006, 99, 066111.	2.5	5
227	Low VT Mo(O,N) metal gate electrodes on HfSiON for sub-45nm pMOSFET Devices. , 2006, , .		1
228	Cross-sectional studies of epitaxial growth of InP and GaP nanowires on Si and Ge. , 2005, , 295-298.		2
229	Low-temperature diffusion of high-concentration phosphorus in silicon, a preferential movement toward the surface. Applied Physics Letters, 2005, 86, 081917.	3.3	35
230	Advanced PMOS Device Architecture for Highly-Doped Ultra-Shallow Junctions. Japanese Journal of Applied Physics, 2004, 43, 1778-1783.	1.5	4
231	Thickness and composition of ultrathin SiO2 layers on Si. Journal of Vacuum Science and Technology A: Vacuum, Surfaces and Films, 2004, 22, 1572-1578.	2.1	9
232	Transmission electron microscopy specimen holder for simultaneousin situheating and electrical resistance measurements. Review of Scientific Instruments, 2004, 75, 426-429.	1.3	7
233	In situtransmission electron microscopy analysis of electron beam induced crystallization of amorphous marks in phase-change materials. Journal of Applied Physics, 2004, 96, 3193-3198.	2.5	27
234	Characterization of Thermal and Electrical Stability of MOCVD HfO[sub 2]-HfSiO[sub 4] Dielectric Layers with Polysilicon Electrodes for Advanced CMOS Technologies. Journal of the Electrochemical Society, 2004, 151, G870.	2.9	9

#	Article	IF	CITATIONS
235	HfSiO[sub 4] Dielectric Layers Deposited by ALD Using HfCl[sub 4] and NH[sub 2](CH[sub 2])[sub 3]Si(OC[sub 2]H[sub 5])[sub 3] Precursors. Journal of the Electrochemical Society, 2004, 151, C716.	2.9	28
236	Epitaxial growth of InP nanowires on germanium. Nature Materials, 2004, 3, 769-773.	27.5	178
237	Critical review of the current status of thickness measurements for ultrathin SiO2 on Si Part V: Results of a CCQM pilot study. Surface and Interface Analysis, 2004, 36, 1269-1303.	1.8	138
238	Electron emission from individual nitrogen-doped multi-walled carbon nanotubes. Chemical Physics Letters, 2004, 396, 126-130.	2.6	45
239	Island growth in the atomic layer deposition of zirconium oxide and aluminum oxide on hydrogen-terminated silicon: Growth mode modeling and transmission electron microscopy. Journal of Applied Physics, 2004, 96, 4878-4889.	2.5	132
240	Structural Characterization of Mesoporous Organosilica Films for Ultralow-kDielectrics. Journal of Physical Chemistry B, 2003, 107, 4280-4289.	2.6	107
241	Synthesis of InP Nanotubes. Journal of the American Chemical Society, 2003, 125, 3440-3441.	13.7	134
242	Monocrystalline InP Nanotubes. Materials Research Society Symposia Proceedings, 2003, 789, 127.	0.1	0
243	Explanation for the leakage current in polycrystalline-silicon thin-film transistors made by Ni-silicide mediated crystallization. Applied Physics Letters, 2002, 81, 3404-3406.	3.3	49
244	Development of a Rubber Coated Mineral Fiber for Disc Pad Applications. , 2002, , .		0
245	In situ electrical resistance measurements of Al-Ge films in the TEM using a modified heating holder. Materials Research Society Symposia Proceedings, 2000, 615, 611.	0.1	1
246	Difference between Blocking and Néel Temperatures in the Exchange BiasedFe3O4/CoOSystem. Physical Review Letters, 2000, 84, 6102-6105.	7.8	226
247	Mechanism of C60 crystal growth from the vapour. Journal of Crystal Growth, 1997, 172, 136-144.	1.5	3
248	In situ topography of the (2 0 0) face of Ϊμ-caprolactam growing from the vapour phase. Journal of Crystal Growth, 1997, 180, 284-292.	1.5	2
249	On the hypomorphism of ADP crystals. Journal of Crystal Growth, 1996, 160, 337-345.	1.5	4
250	The stability of satellite faces on modulated crystals. Journal of Physics Condensed Matter, 1995, 7, 9369-9384.	1.8	1
251	Optical and atomic force microscopy studies of rhombohedral domains in C ₇₀ crystals. Philosophical Magazine A: Physics of Condensed Matter, Structure, Defects and Mechanical Properties, 1995, 72, 1141-1159.	0.6	6
252	Hexagonal close-packed C60. Chemical Physics Letters, 1994, 219, 469-472.	2.6	57

#	Article	IF	CITATIONS
253	Low-temperature structure of solid C70. Chemical Physics Letters, 1994, 223, 323-328.	2.6	56
254	A superspace description for the morphology of modulated crystals: An explanation for the occurrence of faces (hklm). The Philosophical Magazine: Physics of Condensed Matter B, Statistical Mechanics, Electronic, Optical and Magnetic Properties, 1994, 69, 69-82.	0.6	8
255	Structures and phase transitions in C60 and C70 fullerites. Ultramicroscopy, 1993, 51, 168-188.	1.9	21
256	Explanation for the occurrence of {hklm} faces on modulated crystals. Faraday Discussions, 1993, 95, 3.	3.2	4
257	Structural phase transitions in C ₇₀ . Europhysics Letters, 1993, 21, 329-334.	2.0	72
258	Lattice vibrations in crystallineC70. Physical Review B, 1993, 47, 7610-7613.	3.2	58
259	New orientationally ordered low-temperature superstructure in high-purityC60. Physical Review Letters, 1992, 69, 1065-1068.	7.8	80
260	The structure of different phases of pure C70 crystals. Chemical Physics, 1992, 166, 287-297.	1.9	195
261	Morphology of modulated crystals and quasicrystals. Journal Physics D: Applied Physics, 1991, 24, 186-198.	2.8	12
262	Vicinal Si(111) surfaces studied by optical second-harmonic generation: Step-induced anisotropy and surface-bulk discrimination. Physical Review B, 1990, 42, 9263-9266.	3.2	77
263	Enhanced self-assembled monolayer surface coverage by ALD NiO for p-i-n perovskite solar cells. , 0, , .		0
264	Thin Conformal Hole Transport Layers Enabling Highly Efficient Monolithic Perovskite/CIGSe Tandem Solar Cells. , 0, , .		0
265	Operando Spectroscopy Unveils the Catalytic Role of Different Palladium Oxidation States in CO Oxidation on Pd/CeO ₂ Catalysts. Angewandte Chemie, 0, , .	2.0	0
266	Growthâ€Related Formation Mechanism of I3â€Type Basal Stacking Fault in Epitaxially Grown Hexagonal Geâ€2H. Advanced Materials Interfaces, 0, , 2102340.	3.7	0